Tracking the pre-clinical progression of transthyretin amyloid cardiomyopathy using artificial intelligence-enabled electrocardiography and echocardiography

Evangelos K. Oikonomou MD DPhil[a], Veer Sangha BS[a,b], Sumukh Vasisht Shankar MS[a], Andreas Coppi PhD[c], Harlan M. Krumholz MD SM[a,c], Khurram Nasir MD MPH,[d] Edward J. Miller MD PhD[a], Cesia Gallegos-Kattan MD MHS[a], Sadeer Al-Kindi MD,[e] Rohan Khera MD MS[a,c,f,g*]

[a] Section of Cardiovascular Medicine, Department of Internal Medicine, Yale School of Medicine, New Haven, CT, USA

[b] Department of Engineering Science, University of Oxford, Oxford, UK

[c] Center for Outcomes Research and Evaluation, Yale-New Haven Hospital, New Haven, CT, USA

[d] Division of Cardiovascular Prevention and Wellness, Department of Cardiology, Houston Methodist DeBakey Heart & Vascular Center, Houston, TX

[e] Center for Cardiovascular Computational & Precision Health, Houston Methodist DeBakey Heart & Vascular Center, Houston, TX, USA

[f] Section of Biomedical Informatics and Data Science, Yale School of Medicine, New Haven, CT, USA

[g] Section of Health Informatics, Department of Biostatistics, Yale School of Public Health, New Haven, CT, USA

Manuscript type: Original Research Manuscript

Brief title: AI for pre-clinical transthyretin amyloid cardiomyopathy

Word count: 3,134 words**; Figures:** 4**; Tables:** 2

[*]**Correspondence to:** Rohan Khera, MD, MS

195 Church St, 6th Floor, New Haven, CT 06510

203-764-5885; rohan.khera@yale.edu; @rohan_khera

ABSTRACT

Background and Aims: Diagnosing transthyretin amyloid cardiomyopathy (ATTR-CM) requires advanced imaging, precluding large-scale testing for pre-clinical disease. We examined the application of artificial intelligence (AI) to echocardiography (TTE) and electrocardiography (ECG) as a scalable strategy to quantify pre-clinical trends in ATTR-CM.

Methods: Across age/sex-matched case-control datasets in the Yale-New Haven Health System (YNHHS) we trained deep learning models to identify ATTR-CM-specific signatures on TTE videos and ECG images (area under the curve of 0.93 and 0.91, respectively). We deployed these across all studies of individuals referred for cardiac nuclear amyloid imaging in an independent population at YNHHS and an external population from the Houston Methodist Hospitals (HMH) to define longitudinal trends in AI-defined probabilities for ATTR-CM using age/sex-adjusted linear mixed models, and describe discrimination metrics during the early pre-clinical stage.

Results: Among 984 participants referred for cardiac nuclear amyloid imaging at YNHHS (median age 74 years, 44.3% female) and 806 at HMH (69 years, 34.5% female), 112 (11.4%) and 174 (21.6%) tested positive for ATTR-CM, respectively. Across both cohorts and modalities, AI-defined ATTR-CM probabilities derived from 7,423 TTEs and 32,205 ECGs showed significantly faster progression rates in the years before clinical diagnosis in cases versus controls ($p_{\text{time x group interaction}} \leq 0.004$). In the one-to-three-year window before cardiac nuclear amyloid imaging sensitivity/specificity metrics were estimated at 86.2%/44.2% [YNHHS] vs 65.7%/65.5% [HMH] for AI-Echo, and 89.8%/40.6% [YNHHS] vs 88.5%/35.1% [HMH] for AI-ECG.

Conclusions: We demonstrate that AI tools for echocardiographic videos and ECG images can enable scalable identification of pre-clinical ATTR-CM, flagging individuals who may benefit from risk-modifying therapies.

Keywords: cardiac amyloidosis, transthyretin, artificial intelligence, pre-clinical, progression

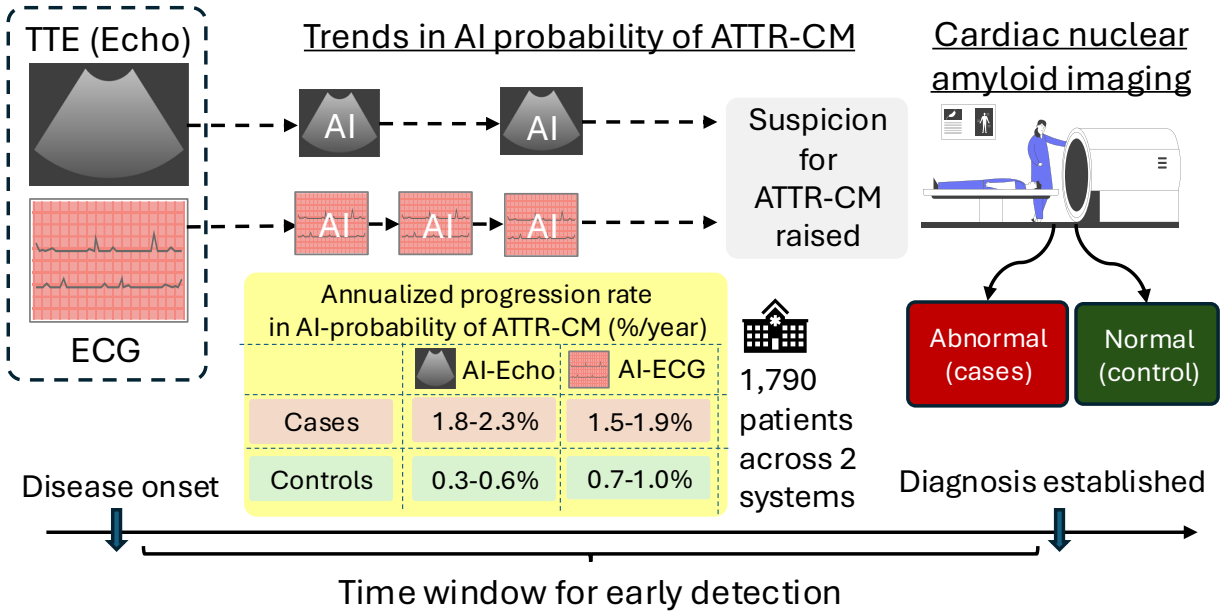

GRAPHICAL ABSTRACT

Key question: Can artificial intelligence (AI) applied to echocardiographic videos and electrocardiographic (ECG) images detect longitudinal changes in pre-clinical transthyretin amyloid cardiomyopathy (ATTR-CM)?

Key finding: Across 1,790 patients referred for cardiac nuclear amyloid imaging in two large and diverse hospital systems, AI probabilities for ATTR-CM exhibited significantly higher annualized progression rates among cases vs controls, with a significant acceleration in the rate of AI-defined progression in the years preceding a clinical diagnosis.

Take-home message: AI applied directly to echocardiography and ECG images may define a scalable paradigm in the monitoring of pre-clinical ATTR-CM progression and identify candidates who may benefit from initiation of disease-modifying therapies.

INTRODUCTION

Awareness of the insidious onset and progression of transthyretin amyloid cardiomyopathy (ATTR-CM) is increasing, with growing recognition of its under-appreciated prevalence and links to incident heart failure and premature mortality.[1–6] This is partly due to the evolution of several new therapeutic agents that can effectively reduce the associated morbidity and mortality.[1,7] These therapies can stabilize abnormally folded transthyretin protein that deposits in myocardium,[8,9] silence its production,[10,11] and even promote its clearance,[12] thereby modifying the course of the disease and effectively reducing the risk of adverse outcomes, especially when deployed early during the disease course. Despite effectiveness, on-treatment mortality and morbidity remain high,[8,9,13] suggesting the need for earlier identification and treatment. The key challenge with optimizing the use of these new therapeutic agents is identifying individuals before the onset of symptoms, long before traditional diagnostic testing is usually performed. While cardiac nuclear amyloid imaging remains a key part of the diagnostic cascade,[1,14] the need for access to specialized centers, its cost, and radiation exposure, limit its broader use in identifying those with pre-clinical disease. Therefore, there are currently no scalable strategies or tools to identify individuals with pre-clinical disease and track its progression to flag the appropriate time for intervention.

In this study, we hypothesized that structural, electrical, and mechanical changes induced by the deposition of misfolded transthyretin are detectable through AI-enhanced interpretation of routine transthoracic echocardiography (TTE) and 12-lead electrocardiography (ECG). These tools may then be deployed to characterize subtle longitudinal changes that forecast the subsequent development of clinical disease. In this multi-cohort study, we explored the ability of AI to phenotype and track longitudinal changes in ATTR-CM-specific signatures on these

accessible modalities during the pre-clinical window that precedes the eventual confirmation of a clinical ATTR-CM diagnosis. To this end, we identified individuals with clinical phenotypes that prompted a clinical referral for cardiac nuclear amyloid imaging, both with and without an eventual diagnosis of ATTR-CM, and described longitudinal trajectories in the AI-assisted interpretation of their echocardiograms and ECGs as a potential screening and monitoring strategy during this early stage (**Figure 1**).

METHODS

Study population and data source

This was a retrospective study across two large and diverse health systems, namely the Yale-New Haven Health System (YNHHS, internal set), spanning 5 hospitals and affiliated clinic sites across Connecticut and Rhode Island, and the geographically distinct Houston Methodist Hospitals (HMH, external testing set, with 8 hospitals and affiliated clinic sites) in Houston, Texas. Across sites, we identified patients 18 years or older and referred for evaluation of ATTR-CM by cardiac nuclear amyloid imaging with an approved bone radiotracer (i.e., Tc^{99m}-pyrophosphate [PYP]). First, we trained standard deep learning models to discriminate between a subset of established ATTR-CM at YNHHS and age- and sex-matched controls without ATTR-CM, extracted from the local echocardiographic and ECG databases. Next, we deployed these models across independent datasets in YNHHS and HMH to assess their ability to track longitudinal changes in the probability of ATTR-CM in patients where clinical suspicion was high enough to trigger a referral for cardiac nuclear amyloid imaging, further stratifying these individuals based on positive vs negative (non-diagnostic) results for ATTR-CM in line with standard guidelines (**Figure 2**).[15] Respective Institutional Review Boards approved the study

protocol and waived the need for informed consent as the study involves secondary analysis of pre-existing data.

Study exposure and outcomes

For training an AI-Echo and AI-ECG classifier for the cross-sectional detection of ATTR-CM, we classified any TTE or ECG studies performed up to one year before or any time after an abnormal cardiac nuclear amyloid imaging study as positive for the ATTR-CM phenotype. This definition ensured the specificity of the label for ATTR-CM and was based on the median delay (latency) in ATTR-CM diagnosis that has been estimated at 12-13 months across contemporary studies.[13,16] Across cohorts, cardiac nuclear amyloid imaging was performed in accordance with the recommendations of the American Society of Nuclear Cardiology with an approved radiotracer (i.e., Tc^{99m}-pyrophosphate [PYP]). The final diagnosis of a positive study was adjudicated by the interpreting physician based on a combination of visual (semi-quantitative) myocardial radiotracer (Tc^{99m}-PYP) uptake corresponding to a Perugini class of ≥2 or a heart-to-contralateral lung ratio of >1.5.[15]

Cross-sectional discrimination of ATTR-CM: AI-Echo and AI-ECG model development

To define an algorithm that learns the unique features of ATTR-CM on echocardiography and ECGs, we first trained deep learning models for direct use with transthoracic echocardiograms (AI-Echo) and electrocardiographic images (AI-ECG) using an age- and sex-matched case-control design for each modality.

AI-Echo model development: Given the lower counts of echocardiograms relative to ECG studies and to ensure that patients with sequential studies were not seen during model

training, participants who had two or more TTE studies before a positive cardiac nuclear amyloid imaging exam were not included in the training or validation of the amyloid detection models. These were reserved for the progression analysis in YNHHS.

The diagnostic model development population included 308 studies from 101 unique individuals, split at a patient level into training and validation sets (80%, 20%) to develop an AI-Echo model for detecting concurrent ATTR-CM.

Age- and sex-matched controls (10 controls per case) were sampled from individuals from the same period without a history of abnormal cardiac nuclear amyloid imaging or transthyretin amyloidosis based on the International Classification of Diseases (ICD) codes (“E85.2", "E85.82"). The AI-Echo model development population is summarized in **Table S1**.

During model development, we followed our previously described end-to-end pre-processing pipeline for echocardiographic studies stored in DICOM (Digital Imaging and Communications in Medicine) format, which involves deidentification, automated view classification steps, as well as standard augmentation by padding, random rotation, and horizontal flipping.[17] We used a 3D ResNet-18 backbone, class-balanced loss function (weighted binary cross-entropy), the Adam optimizer, a learning rate of 10^{-4}, a batch size of 56, a random dropout of 0.25, and label smoothing (=0.1), and trained our algorithm for a maximum of 30 epochs with patience (early stopping) set at 5 epochs. For predictive estimates for the full echocardiographic study, we used key echocardiographic views that included the left ventricle and left atrium (parasternal long axis, and any of the standard apical four-, three- or two-chamber views) as inputs and performed mean averaging of the output probabilities across these views. The full process is described in the **Supplement**.

AI-ECG model development: The AI-ECG image model was trained in line with our previously described approach.[18–20] Furthermore, to increase the accuracy of our labels, we required that all controls had a TTE performed within 15 days of the ECG during training but did not receive a diagnosis of ATTR-CM during follow-up. The AI-ECG development population is summarized in **Table S2**.

Images of ECGs were generated from 12-lead recordings at a frequency of 500 Hz for 10 seconds collected on various machines (i.e., Philips PageWriter machines and GE MAC machines). We followed our previously described approach of standard transformation, calibration, plotting across various lead layout formats, baseline wander correction, and random augmentation.[18] We used an EfficientNet-B3 backbone that was initialized using weights from a self-supervised biometric contrastive learning approach that we have previously defined.[19] We used a class-balanced binary cross-entropy loss function, an Adam optimizer, gradient clipping, a learning rate of 64, a batch size of 10^{-5}. The full process and training population is described in the **Supplement**.

Identification of pre-clinical ATTR-CM progression using AI-Echo and AI-ECG signatures

To explore the ability of the AI-Echo and AI-ECG models to describe serial, longitudinal changes in ATTR-CM probabilities leading up to a clinical diagnosis of ATTR-CM by a positive cardiac nuclear amyloid imaging study, we deployed the models across independent datasets of individuals who had sequential testing before their eventual nuclear cardiology exam. More specifically, the models were independently deployed across two geographically distinct patient populations drawn from

YNHHS (September 2016 through January 2024) and HMH (March 2016 through May 2024). For the ECG analysis at YNHHS, we removed samples that had previously been used during the model's training. We stratified both cohorts based on the results of cardiac nuclear amyloid imaging testing as positive (first positive study for any individuals eventually diagnosed with ATTR-CM) or negative (first negative study, with no established diagnosis by the end of follow-up). Negative cardiac scintigraphy studies represented the controls since clinical suspicion was high enough to prompt referral for dedicated nuclear imaging, but the result of the cardiac scintigraphy study further supported the lack of an ATTR-CM diagnosis.

We directly deployed the AI-Echo and AI-ECG models to all TTE videos and ECG images from these participants with serial testing without further development. Across cohorts, all TTE studies were available in standard DICOM format. In YNHHS, ECG images were available in a standard format as .png files, whereas in HMH, these were exported directly as flattened .pdf files. To ensure transparency during testing in an external population, we embedded both the AI-ECG and AI-Echo models into executable applications that contained standardized environments and enabled direct inference on the TTE and ECG studies at HMH. There was no transfer of patient identifiable data across sites. The software applications can be made available by the authors as part of a research collaboration.

Statistical analysis

Continuous variables are presented as median [25^{th}-75^{th} percentile] and compared using the Mann-Whitney test across two groups. Categorical variables are summarized as counts (and percentages) and compared across distinct groups using the χ^2 test. We summarized the discrimination performance of the AI-Echo and AI-ECG models using the area under the

receiver operating characteristic curve [AUROC] for ATTR-CM with corresponding 95% confidence intervals (CI) derived from bootstrapping with 200 replications.

To assess the differential progression in AI-Echo and AI-ECG output probabilities (0 to 1) for the ATTR-CM phenotype across cardiac scintigraphy-positive vs negative participants, we fit a mixed-effects linear regression model with the AI-Echo or AI-ECG probability of ATTR-CM as the dependent variable, and the following independent variables: cardiac nuclear amyloid imaging status (positive versus negative), the time difference between each ECG/TTE study, their interaction term, the time of cardiac scintigraphy, age at the time of cardiac nuclear amyloid imaging, and sex. Given the correlatedness of observations within each individual, participant was included as a random effect. Summary statistics (means and 95% confidence interval of mean) were also estimated and summarized across discrete time intervals (more than 5 years before cardiac nuclear amyloid imaging, 3 to 5 years before, 1 to 3 years before, last 12 months, or any time after). Patient-level sensitivity and specificity metrics at a fixed threshold of 0.015 are also presented for each cohort, modality, and unique time window, with 95% confidence intervals calculated by bootstrapping, as above. Furthermore, we derived annualized progression rates in the dependent variable (AI probability of ATTR-CM) across cases and controls by extracting the coefficients (and respective standard errors) for time and its interaction with cardiac nuclear amyloid imaging status from the previously fitted mixed linear model. All statistical tests were two-sided with a significance level of 0.05 unless specified otherwise.

RESULTS

Cross-sectional discrimination of ATTR-CM by AI-ECG and AI-Echo

We first independently evaluated the internal performance of the AI-Echo and AI-ECG models in their respective testing sets. In the TTE held-out testing cohort that included 138 TTE cases and 1380 TTE control studies (median age 79 [IQR: 75, 84] years, 1166 [76.8%] male [**Table S1**]), the AI-Echo model reached a study-level AUROC of 0.93 (95%CI: 0.90-0.96). Similarly, in the ECG held-out testing cohort from YNHHS that included 139 ECG cases and 1390 ECG controls (median age 80 [IQR: 75, 86] years, 1,044 [68.3%] male [**Table S2**]) the AI-ECG model successfully discriminated ATTR-CM cases from controls with an AUROC of 0.91 (95%CI: 0.88-0.93).

AI-Echo and AI-ECG to track the pre-clinical progression of ATTR-CM

The AI-Echo and AI-ECG models developed above were independently deployed across the cohorts designed to evaluate the electrocardiographic and echocardiographic lead time before the development of clinical ATTR-CM. There were 4,010 unique TTEs and 22,340 ECGs in 984 unique individuals in the progression cohort at YNHHS, with 112 of these individuals (11.4%) had abnormal findings compatible with ATTR-CM on cardiac nuclear amyloid imaging. At the external site, HMH, there were 3,413 TTEs and 9,865 ECGs in 806 participants, with 174 (21.6%) demonstrating eventual positivity on cardiac nuclear amyloid imaging (**Table 1**). Compared with negative cases, positive cases were older at the time of cardiac nuclear amyloid imaging (YNHHS: 82 [IQR 75, 86] vs 73 [IQR 64, 80] years, and HMH: 77 [IQR 70, 82] vs 67 [IQR 57, 75] years, all $p<0.001$) and more frequently men (YNHHS: n=77 [68.8%] vs n=471 [54.0%], and HMH: n=145 [83.3%] vs n=383 [60.6%], $p<0.001$).

ATTR-CM Progression at YNHHS

In YNHHS, the site where the models were developed but did not include individuals in the progression cohort, we observed a positive and significant association between higher AI-Echo and AI-ECG predictions during the pre-clinical stage and subsequent positivity on cardiac scintigraphy testing, independent of age and sex (**Figure 3**). For AI-Echo, the age- and sex-adjusted annualized progression rate in AI probabilities was estimated at 2.3%/year [95%CI: 1.8%-2.9%/year] among cases vs 0.6%/year [95%CI: 0.5%-0.9%/year] among controls, whereas for AI-ECG the rates were 1.5%/year [95%CI: 1.2%-1.7%/year] vs 0.7%/year [95%CI: 0.6%-0.9%/year], respectively. There was a significant interaction between time and eventual cardiac nuclear amyloid imaging positivity on the rates of progression in AI probabilities (**Table 2**). For instance, when comparing the mean (standard error of mean) probabilities more than 5 years before cardiac scintigraphy to those in the year before diagnosis, AI-Echo and AI-ECG probabilities in cases increased from 0.057±0.025 (AI-Echo; n=21) and 0.075±0.020 (AI-ECG; n=32) to 0.379±0.028 (AI-Echo, n=84) and 0.289±0.026 (AI-ECG, n=62). However, they remained relatively unchanged in controls, from 0.025±0.004 (AI-Echo, n=136) and 0.063±0.005 (AI-ECG, n=466) more than 5 years before cardiac scintigraphy, to 0.077±0.005 (AI-Echo, n=669) and 0.123±0.006 (AI-ECG, n=780) in the year before testing, with the curves between cases and controls separating as early as 3 years before cardiac nuclear amyloid imaging (**Figure 3**). Between three and one years before nuclear amyloid imaging, sensitivity and specificity were 86.2% [95%CI: 76.8%-93.2%] and 44.2% [95%CI: 40.4%-48.9%] for AI-Echo, and 89.8% [95%CI: 81.3%-97.5%] and 40.6% [95%CI: 36.9%-44.0%] for AI-ECG, respectively (**Table S3**).

ATTR-CM Progression at HMH

In external testing in the HMH cohort, the annualized progression rates among cases vs controls were estimated at 1.8% [95%CI: 1.3%-2.3%] vs 0.3% [95%CI: 0.1-0.5%] for AI-Echo, and 1.8% [95%CI: 1.2-2.4%] vs 1.0% [95%CI: 0.7%-1.3%] for AI-ECG (**Figure 4**). Similar to the internal testing set, there was a positive interaction between cardiac nuclear amyloid imaging status and time when assessing their effects on the AI probability of ATTR-CM, suggesting disproportionately faster progression rates among imaging-positive vs -negative cases in the years before their diagnosis (**Table 2**). Between three years and one year before cardiac nuclear amyloid imaging, sensitivity and specificity were 65.7% [95%CI: 46.7%-79.0%] and 65.5% [95%CI: 58.6%-71.3%] for AI-Echo, and 88.5% [95%CI: 78.9%-89.7%] and 35.1% [95%CI: 29.1%-39.8%] for AI-ECG, respectively (**Table S3**).

DISCUSSION

In two large, diverse, and geographically distinct health system-based cohorts, we demonstrate that AI applied to standard TTE videos and ECG images may automate the detection of progressive phenotypic changes that occur during the pre-clinical stages of ATTR-CM. Our findings propose a possible new paradigm in which deep learning-enhanced interpretation of accessible diagnostic tests identifies signals of myocardial remodeling that precede the clinical diagnosis of ATTR-CM by up to 3 years, and which are generalizable across distinct cohorts. These observations provide evidence to support the use of AI-Echo and AI-ECG in identifying at-risk individuals, potentially downstream diagnostic testing, and flagging individuals who may benefit from novel risk-modifying therapies.

Our findings should be interpreted in the context of recent evidence on the changing epidemiological and therapeutic landscape of ATTR-CM. Given advances in the non-invasive

diagnosis by cardiac nuclear amyloid imaging and cardiac magnetic resonance (CMR) imaging, referrals to amyloidosis centers have been increasing. While a U.K.-based study estimated that the median duration of symptoms prior to diagnosis has decreased from 36 months in 2002 to 12 months in 2021,[13] multinational registries demonstrate persistent delays from symptom onset to ATTR-CM diagnosis that often exceed two years.[21] There is also a growing recognition that myocardial ATTR deposition often co-occurs with prevalent conditions, such as aortic stenosis and heart failure with preserved ejection fraction,[2–4] thus highlighting an emerging need for scalable and cost-efficient screening tool that can be deployed serially in at-risk populations.

To date, efforts to develop reliable prognostic biomarkers for ATTR-CM have been hampered by the low prevalence in the community, complex etiological and pathophysiological profile, and substantial heterogeneity across cases. However, rapid advances in the therapeutic landscape of ATTR-CM have revealed a gap in scalable diagnostics to monitor the pre-clinical stages of the condition. Most prognostic markers have been evaluated among patients with an existing diagnosis, such as NT-proBNP (N-terminal pro-Brain Natriuretic Peptide) levels or outpatient intensification of diuretics, which consistently portend worse prognosis among patients with ATTR-CM.[22] Furthermore, while cardiac nuclear amyloid imaging represents an excellent non-invasive alternative to traditional biopsy,[23,24] it is expensive, not widely available, and associated with radiation exposure, all features that preclude its use in longitudinal monitoring. As a result, attention has shifted to maximizing inference from easily scalable modalities performed during initial patient evaluation. AI methods directly applied to ECG signals and TTE videos have shown potential in detecting distinct electrical and structural signatures associated with the cardiac amyloidosis phenotype.[25–27] However, a key gap in our knowledge is whether the signatures described by AI-Echo and AI-ECG can track longitudinal

changes during the pre-clinical stage, a critical period during which early diagnosis and intervention may prevent subsequent morbidity and mortality. This is particularly relevant to individuals with early evidence of left ventricular hypertrophy and related changes in diastolic function, but also phenotypically normal individuals who may be known to harbor pathogenic or likely pathogenic *TTR* variants,[28] where penetrance, age at disease onset, and progression rates may vary substantially.[29]

Our study provides key insights into the possibility of using AI-augmented ECG and TTE interpretation to track serial phenotypic changes of at-risk individuals in the community, possibly forecasting the development of clinical disease and possibly reducing the gap between symptom onset and disease diagnosis. As the potential eligibility pool for new therapies expands further, AI-enabled phenotyping could also guide optimal case selection during this pre-clinical stage and identify individuals who may derive the greatest benefit from early intervention based on an objectively quantifiable and dynamically evolving phenotype. Moreover, since many variant forms (i.e., V122I, pV142I) are more prevalent among traditionally disadvantaged communities, including racial and ethnic monitories (i.e., individuals of African or Hispanic/Latino ancestry), AI-enabled interpretation of accessible diagnostic modalities may also improve access to timely diagnostic care,[30–32] given that they represent the most commonly accessible form of ECGs available to the end-users. With the arrival of a rapidly expanding armamentarium of therapeutic agents that can not only stabilize abnormal TTR, but also inhibit its production in the liver and promote its clearance once deposited in remote organs,[1,7–12] AI-Echo and AI-ECG-enabled screening methods may identify at-risk individuals, guide targeted enrichment in prospective clinical trials, and further expand our knowledge on the pre-clinical stages of the disease, its trajectory, and the ability to modify it.

Limitations: Certain limitations merit consideration. First, this was a retrospective analysis of individuals in whom clinical suspicion for ATTR-CM prompted a referral for dedicated cardiac nuclear amyloid imaging testing. Similarly, ECG and TTE studies performed before or after clinical diagnosis were part of clinical care. As a result, it is unclear whether these findings can generalize to undiagnosed patients with pre-clinical ATTR-CM in the community who were never screened by ECG, TTE, or cardiac nuclear amyloid imaging testing. Second, imaging-negative cases were younger and less likely to be male than their scintigraphy-positive counterparts. Although the longitudinal trends were independent of age and sex, a negative study does not rule out the future development of the disease, particularly if testing was done at very early stages. Third, we relied on cardiac nuclear amyloid imaging with bone-avid radiotracers, such as Tc^{99m}-PYP, which are known to be highly sensitive and specific for ATTR-CM using established quantitative and semi-quantitative thresholds.[24] However, since these studies were performed as part of clinical care there was no consistent multimodal assessment, or histological confirmation. Similarly, there was no consistent genotyping to assess differential trends across variant and wild-type forms of the disease.

CONCLUSIONS

AI technology applied directly to echocardiography and ECG images may enable scalable identification of pre-clinical ATTR-CM. These findings suggest a possible role for AI-enabled interpretation of routinely performed cardiac investigations to flag individuals at high risk of progressing to clinical ATTR-CM.

FUNDING

National Heart, Lung, and Blood Institute of the National Institutes of Health (under awards R01HL167858 and K23HL153775 to RK, and F32HL170592 to EKO), the Doris Duke Charitable Foundation (under award number 2022060 to RK), and BridgeBio (through funding awarded to RK through Yale University).

DISCLOSURE OF INTEREST

R.K. is an Associate Editor of JAMA and receives research support, through Yale, from the Blavatnik Foundation, Bristol-Myers Squibb, Novo Nordisk, and BridgeBio. He is a coinventor of U.S. Provisional Patent Applications 63/177,117, 63/428,569, 63/346,610, 63/484,426, 63/508,315, 63/580,137, 63/606,203, 63/562,335, 18/813,882, and a co-founder of Ensight-AI, Inc and Evidence2Health, LLC. E.K.O. is an academic co-founder of Evidence2Health LLC, and has been a consultant for Ensight-AI, Inc, and Caristo Diagnostics, Ltd. He is a co-inventor in patent applications 18/813,882, 17/720,068, 63/619,241, 63/177,117, 63/580,137, 63/606,203, 63/562,335, US11948230B2, and has received royalty fees for technology licensed through the University of Oxford outside the submitted work. VS is a coinventor of 63/346,610 and 63/484,426, and a co-founder of Ensight-AI, Inc. H.M.K. works under contract with the Centers for Medicare & Medicaid Services to support quality measurement programs, was a recipient of a research grant from Johnson & Johnson, through Yale University, to support clinical trial data sharing; was a recipient of a research agreement, through Yale University, from the Shenzhen Center for Health Information for work to advance intelligent disease prevention and health promotion; collaborates with the National Center for Cardiovascular Diseases in Beijing; receives payment from the Arnold & Porter Law Firm for work related to the Sanofi clopidogrel

litigation, from the Martin Baughman Law Firm for work related to the Cook Celect IVC filter litigation, and from the Siegfried and Jensen Law Firm for work related to Vioxx litigation; chairs a Cardiac Scientific Advisory Board for UnitedHealth; was a member of the IBM Watson Health Life Sciences Board; is a member of the Advisory Board for Element Science, the Advisory Board for Facebook, and the Physician Advisory Board for Aetna; and is the co-founder of Hugo Health, a personal health information platform, and co-founder of Refactor Health, a healthcare AI-augmented data management company, and Ensight-AI, Inc. All other authors declare no competing interests.

DATA AVAILABILITY STATEMENT

The underlying data represent protected health information. To protect patient privacy, the local Institutional Review Boards within each center do not allow the sharing of these data. However, the AI-ECG and AI-TTE models can be made available for research by contacting the corresponding author.

REFERENCES

1. Writing Committee, Kittleson MM, Ruberg FL, Ambardekar AV, Brannagan TH, Cheng RK, et al. 2023 ACC Expert Consensus Decision Pathway on Comprehensive Multidisciplinary Care for the Patient With Cardiac Amyloidosis: A Report of the American College of Cardiology Solution Set Oversight Committee. *J Am Coll Cardiol* 2023;**81**:1076–1126.

2. Tanskanen M, Peuralinna T, Polvikoski T, Notkola I-L, Sulkava R, Hardy J, et al. Senile systemic amyloidosis affects 25% of the very aged and associates with genetic variation in alpha2-macroglobulin and tau: a population-based autopsy study. *Ann Med* 2008;**40**:232–239.

3. Scully PR, Treibel TA, Fontana M, Lloyd G, Mullen M, Pugliese F, et al. Prevalence of Cardiac Amyloidosis in Patients Referred for Transcatheter Aortic Valve Replacement. *J Am Coll Cardiol* 2018;**71**:463–464.

4. Castaño A, Narotsky DL, Hamid N, Khalique OK, Morgenstern R, DeLuca A, et al. Unveiling transthyretin cardiac amyloidosis and its predictors among elderly patients with severe aortic stenosis undergoing transcatheter aortic valve replacement. *Eur Heart J* 2017;**38**:2879–2887.

5. AbouEzzeddine OF, Davies DR, Scott CG, Fayyaz AU, Askew JW, McKie PM, et al. Prevalence of Transthyretin Amyloid Cardiomyopathy in Heart Failure With Preserved Ejection Fraction. *JAMA Cardiol* 2021;**6**:1267–1274.

6. González-López E, Gallego-Delgado M, Guzzo-Merello G, Haro-Del Moral FJ de, Cobo-Marcos M, Robles C, et al. Wild-type transthyretin amyloidosis as a cause of heart failure with preserved ejection fraction. *Eur Heart J* 2015;**36**:2585–2594.

7. Kittleson MM, Maurer MS, Ambardekar AV, Bullock-Palmer RP, Chang PP, Eisen HJ, et al. Cardiac Amyloidosis: Evolving Diagnosis and Management: A Scientific Statement From the American Heart Association. *Circulation* 2020;**142**:e7–e22.

8. Maurer MS, Schwartz JH, Gundapaneni B, Elliott PM, Merlini G, Waddington-Cruz M, et al. Tafamidis Treatment for Patients with Transthyretin Amyloid Cardiomyopathy. *N Engl J Med* 2018;**379**:1007–1016.

9. Gillmore JD, Judge DP, Cappelli F, Fontana M, Garcia-Pavia P, Gibbs S, et al. Efficacy and Safety of Acoramidis in Transthyretin Amyloid Cardiomyopathy. *N Engl J Med* 2024;**390**:132–142.

10. Maurer MS, Kale P, Fontana M, Berk JL, Grogan M, Gustafsson F, et al. Patisiran Treatment in Patients with Transthyretin Cardiac Amyloidosis. *N Engl J Med* 2023;**389**:1553–1565.

11. Benson Merrill D., Waddington-Cruz Márcia, Berk John L., Polydefkis Michael, Dyck Peter J., Wang Annabel K., et al. Inotersen Treatment for Patients with Hereditary Transthyretin Amyloidosis. *N Engl J Med* Massachusetts Medical Society; 2018;**379**:22–31.

12. Garcia-Pavia Pablo, aus dem Siepen Fabian, Donal Erwan, Lairez Olivier, van der Meer Peter, Kristen Arnt V., et al. Phase 1 Trial of Antibody NI006 for Depletion of Cardiac Transthyretin Amyloid. *N Engl J Med* Massachusetts Medical Society; 2023;**389**:239–250.

13. Ioannou A, Patel RK, Razvi Y, Porcari A, Sinagra G, Venneri L, et al. Impact of Earlier Diagnosis in Cardiac ATTR Amyloidosis Over the Course of 20 Years. *Circulation* 2022;**146**:1657–1670.

14. Spielvogel CP, Haberl D, Mascherbauer K, Ning J, Kluge K, Traub-Weidinger T, et al. Diagnosis and prognosis of abnormal cardiac scintigraphy uptake suggestive of cardiac amyloidosis using artificial intelligence: a retrospective, international, multicentre, cross-tracer development and validation study. *Lancet Digit Health* 2024;**6**:e251–e260.

15. Dorbala S, Ando Y, Bokhari S, Dispenzieri A, Falk RH, Ferrari VA, et al. ASNC/AHA/ASE/EANM/HFSA/ISA/SCMR/SNMMI Expert Consensus Recommendations for Multimodality Imaging in Cardiac Amyloidosis: Part 1 of 2-Evidence Base and Standardized Methods of Imaging. *Circ Cardiovasc Imaging* 2021;**14**:e000029.

16. Ladefoged B, Dybro A, Povlsen JA, Vase H, Clemmensen TS, Poulsen SH. Diagnostic delay in wild type transthyretin cardiac amyloidosis - A clinical challenge. *Int J Cardiol* 2020;**304**:138–143.

17. Holste G, Oikonomou EK, Mortazavi BJ, Coppi A, Faridi KF, Miller EJ, et al. Severe aortic stenosis detection by deep learning applied to echocardiography. *Eur Heart J* 2023;

18. Sangha V, Nargesi AA, Dhingra LS, Khunte A, Mortazavi BJ, Ribeiro AH, et al. Detection of Left Ventricular Systolic Dysfunction From Electrocardiographic Images. *Circulation* 2023;

19. Sangha V, Khunte A, Holste G, Mortazavi BJ, Wang Z, Oikonomou EK, et al. Biometric contrastive learning for data-efficient deep learning from electrocardiographic images. *J Am Med Inform Assoc* 2024;

20. Sangha V, Mortazavi BJ, Haimovich AD, Ribeiro AH, Brandt CA, Jacoby DL, et al. Automated multilabel diagnosis on electrocardiographic images and signals. *Nat Commun* 2022;**13**:1583.

21. Coelho T, Dispenzieri A, Grogan M, Conceição I, Waddington-Cruz M, Kristen AV, et al. Patients with transthyretin amyloidosis enrolled in THAOS between 2018 and 2021 continue to experience substantial diagnostic delay. *Amyloid* 2023;**30**:445–448.

22. Ioannou A, Cappelli F, Emdin M, Nitsche C, Longhi S, Masri A, et al. Stratifying Disease Progression in Patients With Cardiac ATTR Amyloidosis. *J Am Coll Cardiol* 2024;**83**:1276–1291.

23. Rauf MU, Hawkins PN, Cappelli F, Perfetto F, Zampieri M, Argiro A, et al. Tc-99m labelled bone scintigraphy in suspected cardiac amyloidosis. *Eur Heart J* 2023;**44**:2187–2198.

24. Bokhari S, Castaño A, Pozniakoff T, Deslisle S, Latif F, Maurer MS. 99mTc-Pyrophosphate Scintigraphy for Differentiating Light-Chain Cardiac Amyloidosis From the Transthyretin-Related Familial and Senile Cardiac Amyloidoses. *Circ Cardiovasc Imaging* American Heart Association; 2013;**6**:195–201.

25. Duffy G, Cheng PP, Yuan N, He B, Kwan AC, Shun-Shin MJ, et al. High-Throughput Precision Phenotyping of Left Ventricular Hypertrophy With Cardiovascular Deep Learning. *JAMA Cardiol* 2022;**7**:386–395.

26. Goto S, Mahara K, Beussink-Nelson L, Ikura H, Katsumata Y, Endo J, et al. Artificial intelligence-enabled fully automated detection of cardiac amyloidosis using electrocardiograms and echocardiograms. *Nat Commun* 2021;**12**:2726.

27. Grogan M, Lopez-Jimenez F, Cohen-Shelly M, Dispenzieri A, Attia ZI, Abou Ezzedine OF, et al. Artificial Intelligence-Enhanced Electrocardiogram for the Early Detection of Cardiac Amyloidosis. *Mayo Clin Proc* 2021;**96**:2768–2778.

28. Carry Brendan J., Young Katelyn, Fielden Samuel, Kelly Melissa A., Sturm Amy C., Avila J. David, et al. Genomic Screening for Pathogenic Transthyretin Variants Finds Evidence of Underdiagnosed Amyloid Cardiomyopathy From Health Records. *JACC: CardioOncology* American College of Cardiology Foundation; 2021;**3**:550–561.

29. Chandrashekar P, Alhuneafat L, Mannello M, Al-Rashdan L, Kim MM, Dungu J, et al. Prevalence and outcomes of p.Val142Ile TTR amyloidosis cardiomyopathy: A systematic review. *Circ Genom Precis Med* Ovid Technologies (Wolters Kluwer Health); 2021;**14**:e003356.

30. Damrauer SM, Chaudhary K, Cho JH, Liang LW, Argulian E, Chan L, et al. Association of the V122I Hereditary Transthyretin Amyloidosis Genetic Variant With Heart Failure Among Individuals of African or Hispanic/Latino Ancestry. *JAMA* 2019;**322**:2191–2202.

31. Selvaraj S, Claggett BL, Quarta CC, Yu B, Inciardi RM, Buxbaum JN, et al. Age Dependency of Cardiovascular Outcomes With the Amyloidogenic pV142I Transthyretin Variant Among Black Individuals in the US. *JAMA Cardiol* 2023;**8**:784–788.

32. Selvaraj S, Claggett B, Shah SH, Mentz RJ, Khouri MG, Manichaikul AW, et al. Cardiovascular Burden of the V142I Transthyretin Variant. *JAMA* 2024;**331**:1824–1833.

TABLES

Table 1 | Participant-level demographics for progression analysis.

		YNHHS (internal)		HMH (external)	
Nuclear amyloid imaging status		**Negative**	**Positive**	**Negative**	**Positive**
Total participants (n)		872	112	632	174
Age at nuclear imaging (years)		73 [64, 80]	82 [75, 86]	67 [57-75]	77 [70-82]
Gender	*Female*	401 (46.0)	35 (31.3)	249 (39.4)	29 (16.7)
	Male	471 (54.0)	77 (68.8)	383 (60.6)	145 (83.3)
Race	*Asian*	7 (0.8)	0 (0)	11 (1.7)	3 (1.7)
	Black	245 (28.1)	31 (27.7)	279 (44.1)	70 (40.2)
	White	577 (66.3)	77 (68.8)	324 (51.3)	97 (55.7)
	Other	26 (3.0)	2 (1.8)	11 (1.7)	2 (1.2)
	Unknown	17 (1.9)	2 (1.8)	7 (1.1)	2 (1.2)
Ethnicity	*Hispanic*	32 (3.7)	6 (5.4)	54 (8.5)	8 (4.6)
	Non-Hispanic	819 (93.9)	105 (93.8)	576 (91.1)	163 (93.7)
	Unknown	21 (2.4)	1 (0.9)	2 (0.3)	3 (1.7)
Participants in the TTE sub-study		872 (100)	112 (100)	551 (87.2)	144 (82.8)
TTE study count per patient		3 [2, 5]	3 [2, 6]	8 [5-13]	6 [3-10]
Participants in the ECG sub-study		857 (98.3)	71 (63.3)	632 (100)	174 (100)
ECG study count per patient		17 [7, 32]	11 [4, 21]	9 [4-17]	7 [3-13]

Summary statistics are presented as counts (n) with valid percentages (%) or median [25th 75th percentile]. ECG: electrocardiography; HMH: Houston Methodist Hospital; TTE: transthoracic echocardiography; YNHHS: Yale-New Haven Health System.

Table 2 | Marginal effects of interaction between eventual cardiac nuclear amyloid imaging positivity and time on AI probability of ATTR-CM.

	Yale-New Haven Health System (YNHHS)		Houston Methodist Hospitals (HMH)	
	AI-Echo (n=984 patients)	**AI-ECG (n=928 patients)**	**AI-Echo (n=695 patients)**	**AI-ECG (n=806 patients)**
Cardiac nuclear amyloid imaging result (positive, vs negative)	**0.25 [0.22-0.27], *p*<0.001**	**0.13 [0.10-0.16], *p*<0.001**	**0.22 [0.20-0.25], *p*<0.001**	**0.13 [0.10-0.15], *p*<0.001**
Age at cardiac nuclear amyloid imaging (per 10 year incr.)	0.00 [-0.01, 0.01], *p*=0.64	0.02 [0.02-0.03], *p*<0.001	-0.01 [-0.01, 0.00], *p*=0.14	0.02 [0.01-0.02], *p*=0.001
Sex (male, vs female)	-0.01 [-0.02-0.01], *p*=0.63	0.05 [0.03-0.06], *p*<0.001	0.02 [0.00-0.05], *p*=0.027	0.06 [0.03-0.08], *p*<0.001
Time between study and cardiac nuclear amyloid imaging (per 10-year incr.)	0.07 [0.05-0.09], *p*<0.001	0.07 [0.06-0.09], *p*<0.001	0.03 [0.01-0.05], *p*=0.001	0.10 [0.07-0.13], *p*<0.001
Interaction between cardiac nuclear amyloid imaging result *x* time	**0.16 [0.11-0.22], *p*<0.001**	**0.08 [0.05-0.10], *p*<0.001**	**0.15 [0.10-0.20], *p*<0.001**	**0.08 [0.03-0.13], *p*=0.004**

Results from mixed linear model regression with AI-derived ATTR-CM predictions (0 through 1) as the dependent variable, and cardiac nuclear amyloid imaging status (positive versus negative), age at cardiac nuclear amyloid imaging testing, sex, time difference between echocardiography (or ECG) and cardiac nuclear amyloid imaging test and a time *x* cardiac nuclear amyloid imaging status interaction term as independent fixed effects, and participant as a random effect. ATTR-CM: transthyretin amyloid cardiomyopathy; ECG: electrocardiography.

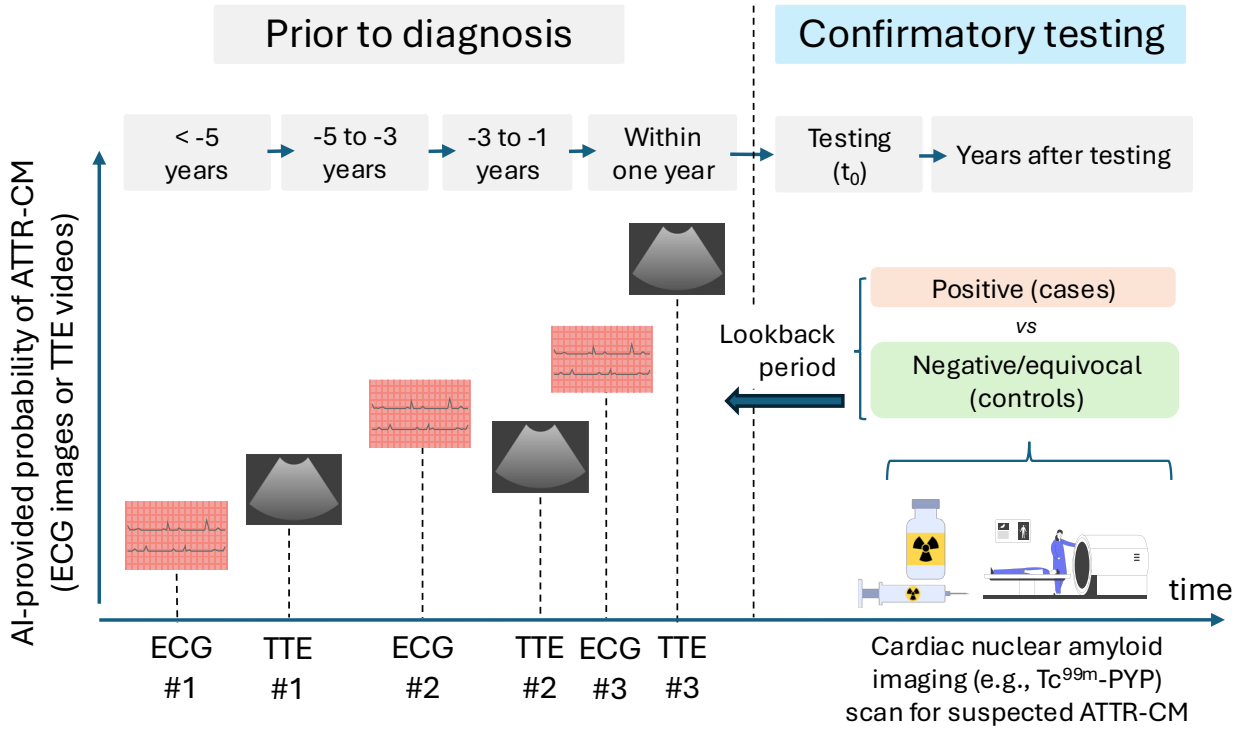

Figure 1 | Study Overview. Deep learning algorithms were trained to discriminate cardiac nuclear amyloid imaging-positive cases of ATTR-CM from age- and sex-matched controls using standard TTE videos or ECG images. These were subsequently deployed across independent sets of patients with longitudinal monitoring by TTE or ECG pre-dating their referral for cardiac nuclear amyloid imaging testing. The overall objective was to examine the ability of the AI models to detect changes in TTE or ECG signatures that precede clinical disease and diagnosis. Such AI-enabled TTE or ECG signatures may be used to forecast the development of ATTR-CM, thus offering a standardized and scalable platform for longitudinal monitoring and screening in the community. AI: artificial intelligence; ATTR-CM: transthyretin amyloid cardiomyopathy; ECG: electrocardiography; Tc^{99m}-PYP: pyrophosphate (cardiac nuclear amyloid imaging tracer); TTE: transthoracic echocardiography.

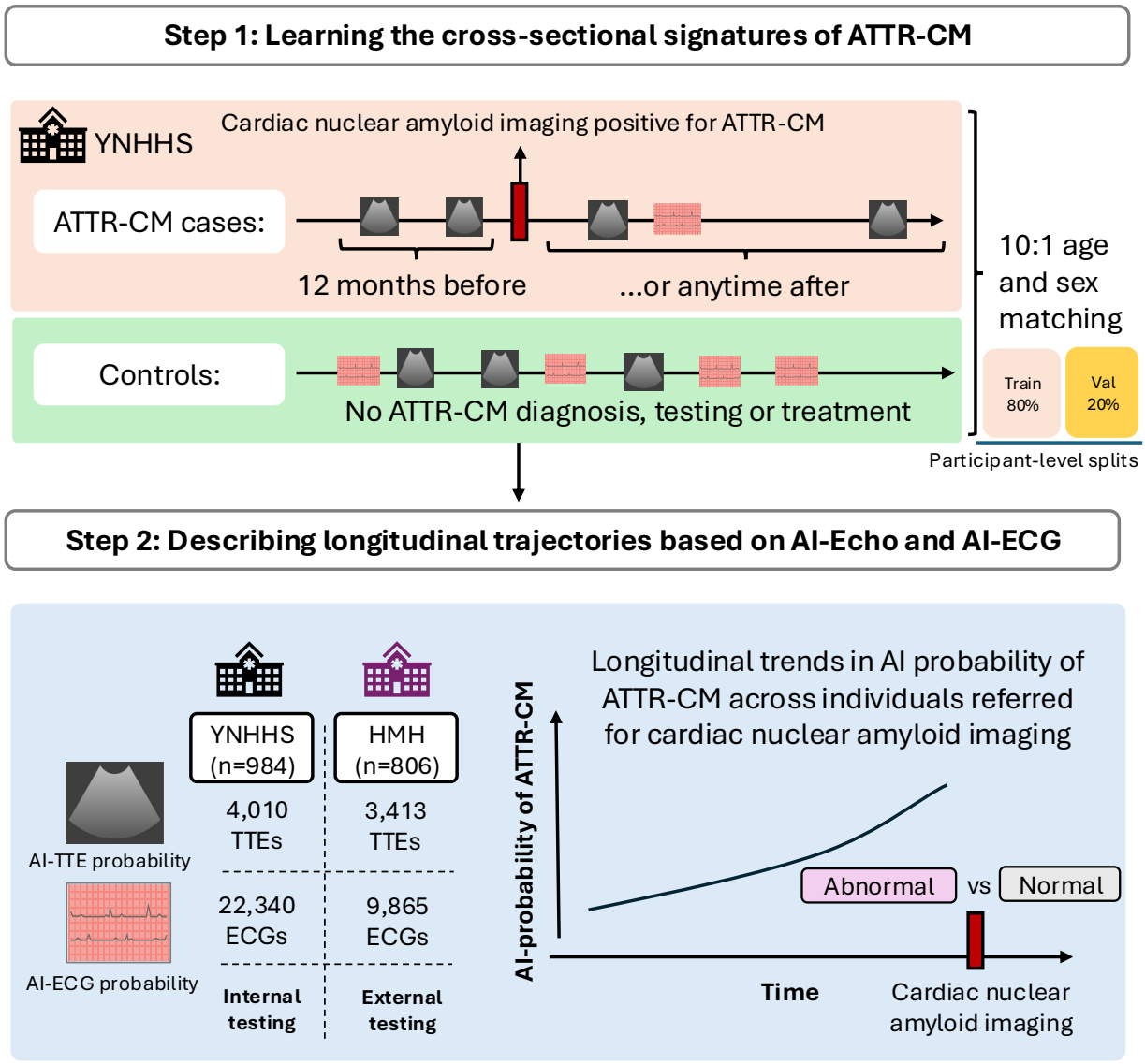

Figure 2 | Study dataset summary. AI-models were trained on transthoracic echocardiograms (TTE) and 12-lead electrocardiographic (ECG) images from patients with ATTR-CM (based on a positive cardiac nuclear amyloid imaging study done within 12 months, or anytime in the past) as well as age- and sex-matched controls across the Yale-New Haven Health System (YNHHS). Models were subsequently deployed across independent sets of patients in YNHHS, as well as an external set of patients from Houston Methodist Hospitals (HMH) who had sequential TTE or ECG performed in the years leading up to confirmatory testing by cardiac nuclear amyloid imaging. This design evaluated the progression of AI-Echo or AI-ECG probabilities as non-invasive markers of pre-clinical ATTR-CM progression. AI: artificial intelligence; ATTR-CM: transthyretin amyloid cardiomyopathy; ECG: electrocardiography; HMH: Houston Methodist Hospitals; Tc^{99m}-PYP: pyrophosphate (cardiac nuclear amyloid imaging tracer); TTE: transthoracic echocardiography; YNHHS: Yale-New Haven Health System.

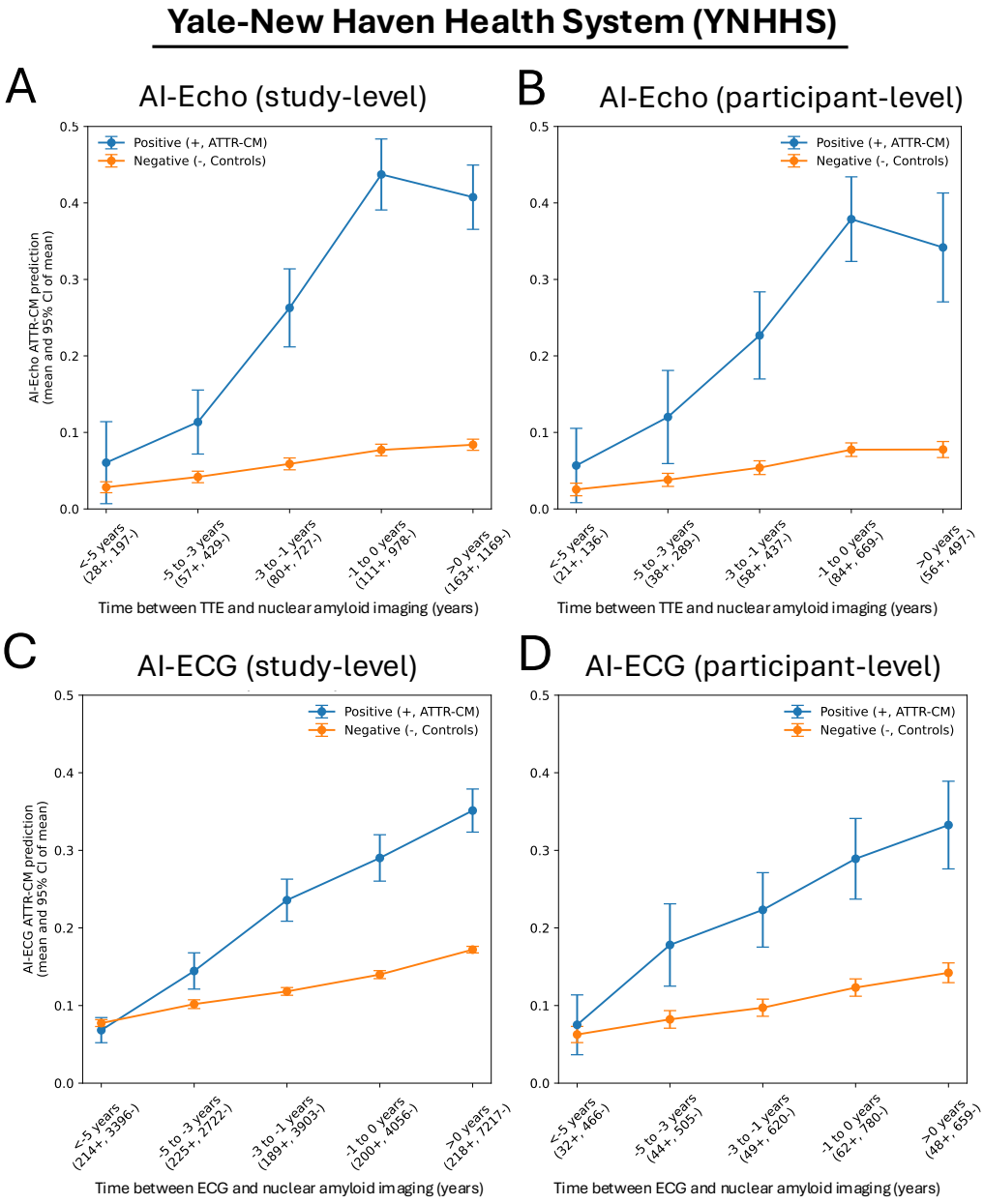

Figure 3 | Longitudinal changes in AI-Echo and AI-ECG ATTR-CM probabilities in the YNHHS population stratified by cardiac nuclear amyloid imaging positivity. The panels illustrate the mean (with error bars denoting the 95% confidence interval of mean) of the AI-Echo (**A, B**) and AI-ECG-derived probabilities (**C, D**) across patients who went on to have a positive (blue color) vs negative (orange color) cardiac nuclear amyloid imaging study. The x axis denotes the time between the TTE/ECG and the timing of the cardiac nuclear amyloid imaging study, summarized across discrete time groups (negative time differences suggest that the TTE/ECG was performed before cardiac nuclear amyloid imaging). The brackets below each period along the x axis denote the number of positive and negative studies or patients. Results are presented both at the study-level (**A, C**), as well as at a participant level (**B, D**) by taking the chronologically last prediction for each unique individual in each period. ATTR-CM: transthyretin amyloid cardiomyopathy; ECG: electrocardiography; TTE: transthoracic echocardiography; YNHHS: Yale-New Haven Health System.

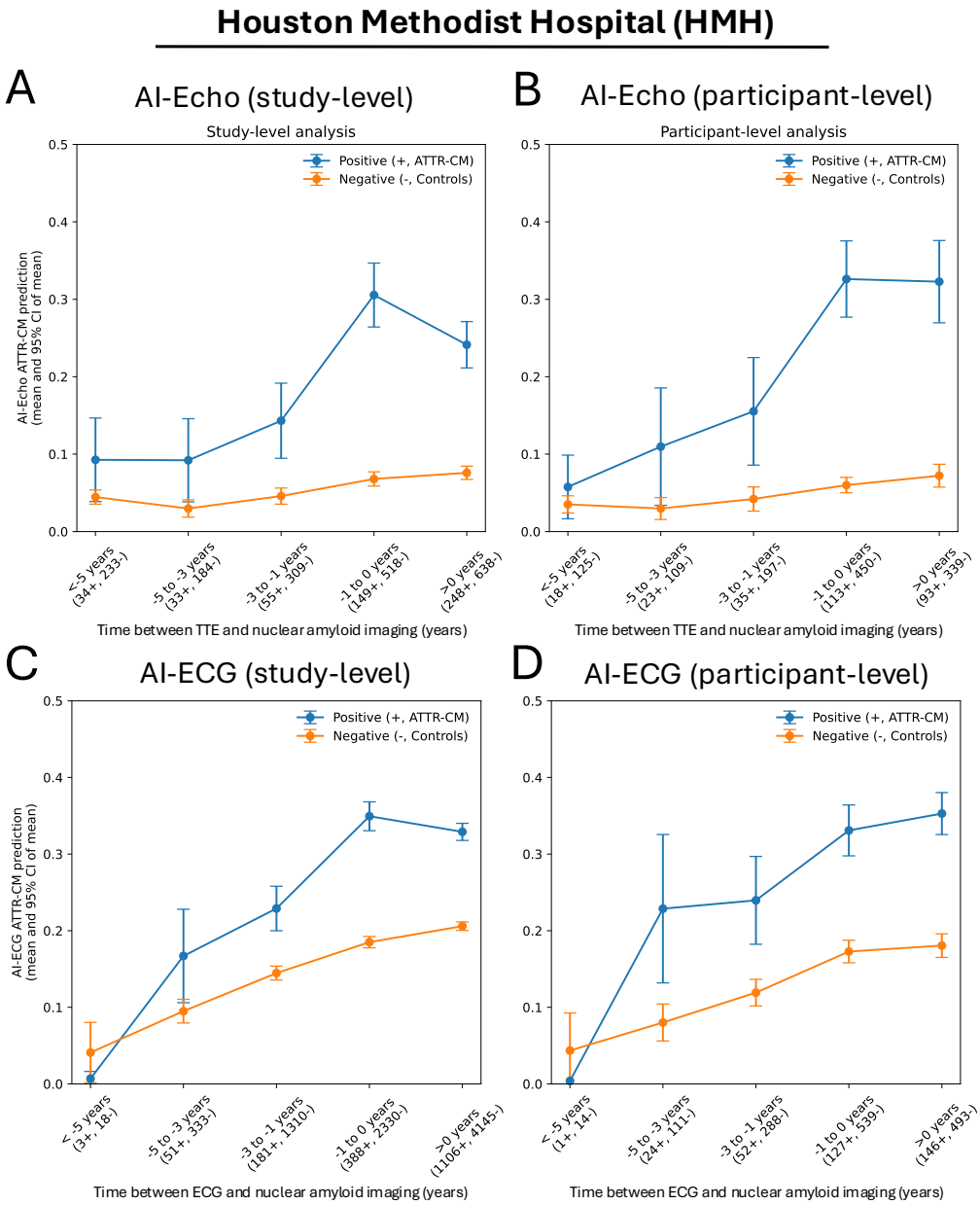

Figure 4 | Longitudinal changes in AI-Echo and AI-ECG ATTR-CM probabilities in the HMH population stratified by cardiac nuclear amyloid imaging positivity. The panels illustrate the mean (with error bars denoting the 95% confidence interval of mean) of the AI-Echo (**A, B**) and AI-ECG-derived probabilities (**C, D**) across patients who went on to have a positive (blue color) vs negative (orange color) cardiac nuclear amyloid imaging study. The x axis denotes the time between the TTE/ECG and the timing of the cardiac nuclear amyloid imaging study, summarized across discrete time groups (negative time differences suggest that the TTE/ECG was performed before cardiac nuclear amyloid imaging). The brackets below each period along the x axis denote the number of positive and negative studies or patients. Results are presented both at the study-level (**A, C**), as well as at a participant level (**B, D**) by taking the chronologically last prediction for each unique individual in each period. ATTR-CM: transthyretin amyloid cardiomyopathy; ECG: electrocardiography; HMH: Houston Methodist Hospital; TTE: transthoracic echocardiography.